A Model to Explore the Interaction Between Muscle Insulin Resistance and β-Cell Dysfunction in the Development of Type 2 Diabetes

Franck Mauvais-Jarvis, Antti Virkamaki, M. Dodson Michael, Jonathon N. Winnay, Ariel Zisman, Rohit N. Kulkarni, and C. Ronald Kahn

Type 2 diabetes is a polygenic disease characterized by defects in both insulin secretion and insulin action. We have previously reported that isolated insulin resistance in muscle by a tissue-specific insulin receptor knockout (MIRKO mouse) is not sufficient to alter glucose homeostasis, whereas β-cell–specific insulin receptor knockout (βIRKO) mice manifest severe progressive glucose intolerance due to loss of glucose-stimulated acute-phase insulin release. To explore the interaction between insulin resistance in muscle and altered insulin secretion, we created a double tissue-specific insulin receptor knockout in these tissues. Surprisingly, βIRKO-MIRKO mice show an improvement rather than a deterioration of glucose tolerance when compared to βIRKO mice. This is due to improved glucose-stimulated acute insulin release and redistribution of substrates with increased glucose uptake in adipose tissue and liver in vivo, without a significant decrease in muscle glucose uptake. Thus, insulin resistance in muscle leads to improved glucose-stimulated first-phase insulin secretion from β-cells and shunting of substrates to nonmuscle tissues, collectively leading to improved glucose tolerance. These data suggest that muscle, either via changes in substrate availability or by acting as an endocrine tissue, communicates with and regulates insulin sensitivity in other tissues. *Diabetes* 49:2126–2134, 2000

Type 2 diabetes is the most common endocrine disorder characterized by impaired insulin-stimulated glucose uptake in skeletal muscle and adipose tissue, increased hepatic glucose production, and inadequate compensation by the pancreatic β-cells, ultimately leading to fasting hyperglycemia (1,2). To clarify the pathogenesis of type 2 diabetes, we and others have disrupted genes for proteins involved in the insulin-signaling cascade in mice, including the insulin receptor (IR) (3,4), insulin receptor substrate (IRS)-1 (5,6) and IRS-2 (7), and the insulin-sensitive glucose transporter GLUT4 (8). This research has provided important insights into the role of each of these proteins in insulin action.

More recently, we have developed genetic models to assess the contribution of individual insulin-sensitive tissues to glucose homeostasis and to the development of type 2 diabetes using the Cre-loxP–mediated recombination strategy to inactivate the IR gene in a tissue-specific fashion. Although insulin resistance in muscle is an early defect in the pathogenesis of type 2 diabetes, muscle-specific insulin receptor knockout (MIRKO) mice show no alteration in glucose homeostasis, but rather manifest alterations in circulating triglycerides, free fatty acid (FFA) levels, and fat mass (9). In contrast, the pancreatic β-cell insulin receptor knockout (βIRKO) mice exhibit a selective loss of acute insulin release in response to glucose, resulting in a progressive impairment of glucose tolerance (10). Because type 2 diabetes is characterized by a combination of insulin resistance in skeletal muscle and impaired insulin secretion from pancreatic β-cells, we have generated a double tissue-specific knockout of the insulin receptor in the pancreatic β-cell and in skeletal muscle (βIRKO-MIRKO) to determine if these defects might synergize or alter the phenotype of the individual tissue defects.

RESEARCH DESIGN AND METHODS

Creation of mutant mice and polymerase chain reaction genotyping. Creation of MIRKO mice and βIRKO mice (i.e., mice homozygous for the IR lox sites, but carrying either the MCK-*Cre* or RIP-*Cre* transgene) has been described previously (9,10). The IR(lox/lox) mouse (carrying the IR allele with loxP sites flanking exon 4) was bred with the MCK-*Cre* transgenic mouse and the RIP-*Cre* transgenic mouse to generate MIRKO and βIRKO mice respectively. To generate the double knockout (βIRKO-MIRKO) mouse, βIRKO mice were bred with MIRKO mice. The resulting F1 generation led to four different genotypes on a similar mixed genetic background: control mice [IR(lox/lox)], MIRKO mice [IR(lox/lox): MCK-*Cre* (+/–)], βIRKO mice [IR(lox/lox: RIP-*Cre* (+/–)], and βIRKO -MIRKO mice [IR(lox/lox): MCK-*Cre* (+/–): RIP-*Cre* (+/–)]. To homogenize the genetic background, the F1 generation was used for multiple breedings to obtain the F2 generation. Among breeders, a given male was never bred with the same female twice. No other mouse was introduced in the breeding scheme. All genotyping was performed by polymerase chain reaction (PCR) using genomic DNA from tail biopsies of 3- to 4-week-old mice. The sequence of the 5′ primer used to identify the presence of the MCK-*Cre* transgene is AGA TGA CCT TGA ACT GCT GG. The sequence of the 5′ primer used to identify the presence of the RIP-*Cre* transgene is CTC TGG CCA TCT GCT GAT CC. The sequence of the 3′ primer, designed from the Cre sequence, is common for both: CGC GCC TGA AGA TAT AGA AG.

From the Research Division, Joslin Diabetes Center and Department of Medicine, Harvard Medical School, Boston, Massachusetts.

Address correspondence and reprint requests to C. Ronald Kahn, Research Division, Joslin Diabetes Center, One Joslin Place, Boston, MA 02215. E-mail: c.ronald.kahn@joslin.harvard.edu.

Received for publication 8 March 2000 and accepted in revised form 30 August 2000.

2-DG, 2-[^{3}H]deoxyglucose; 2-DG-6-P, [^{3}H]-deoxyglucose-6-phosphate; AUC, area under the curve; ELISA, enzyme-linked immunosorbent assay; FFA, free fatty acid; GSA, glucose specific activity; GSIS, glucose stimulation of insulin secretion; GTT, glucose tolerance test; IPGTT, intraperitoneal glucose tolerance test; IR, insulin receptor; IRS, insulin receptor substrate; ITT, insulin tolerance test; PCR, polymerase chain reaction.

All animals were housed on a 12-h light/dark cycle and were fed a standard rodent chow (Purina Mills). All protocols for animal use were reviewed and approved by the Animal Care Committee of the Joslin Diabetes Center and were in accordance with National Institutes of Health guidelines.

Metabolic studies. For glucose tolerance tests (GTTs), glucose stimulation of insulin secretion (GSIS), insulin tolerance tests (ITTs), and random fed blood glucose measurement, blood samples were obtained from mouse tails using heparinized microcapillaries, spun down immediately, and serum was extracted. For GTTs, blood samples were obtained at 0, 15, 30, 60, and 120 min after injection of 2 g/kg dextrose i.p. For GSIS, blood samples were obtained at 0, 2, 5, 15, and 30 min after injection of 3 g/kg dextrose i.p. Blood glucose values were determined from whole venous blood using an automatic glucose monitor (One Touch II, Lifescan). Insulin and leptin levels were measured in serum by enzyme-linked immunosorbent assay (ELISA) using mouse standards (Crystal Chem, Chicago, IL). To assess lipid levels, blood samples were obtained by retro-orbital bleeds from overnight-fasted anesthetized mice. Triglyceride levels were measured in serum by colorimetric assay (Sigma), and FFA levels were determined using the NEFA-kit-U (Amano Enzyme, Osaka, Japan).

Tissue-specific 2-[^{3}H]deoxyglucose uptake during the GTT. To determine the fate of glucose during a GTT, we characterized the tissue distribution of glucose uptake using the nonmetabolizable glucose analog tracer 2-[^{3}H]deoxyglucose (2-DG). 2-DG has been widely used as a tracer to determine tissue glucose uptake because it is trapped inside the tissues after phosphorylation in [^{3}H]-deoxyglucose-6-phosphate (2-DG-6-P). 2-DG (Amersham, Arlington Heights, IL) (8–10 µCi/mouse) was mixed with 20% dextrose to obtain a fixed specific activity before intraperitoneal injection (2 g glucose/kg body wt). To determine the plasma [^{3}H]-radioactivity decay and glucose specific activity (GSA), 15-µl blood samples were obtained from the tail at 0, 15, 30, 60, 90, and 120 min, after which the animals were killed by overdose of pentobarbital, and tissues of interest were snap-frozen in liquid nitrogen. Next, 3 µl of plasma was deproteinized in 3.5% ice-cold perchloric acid (200 µl) for 15 min and centrifuged. After neutralization with 1/4 vol of 2.2-mol $KHCO_3$, the supernatant was counted for [^{3}H]-radioactivity (Beckman LS 6500, Fullerton, CA) and the glucose concentration was measured microfluorometrically (11). The GSA (disintegrations per minute per micromole) was calculated by dividing sample radioactivity by glucose concentration. The mean GSA was determined by dividing the GSA area under the curve (AUC) by the duration of the experiment (120 min).

Tissue-specific accumulation of 2-DG-6-P was determined as previously described, with minor modifications (12). Briefly, 100–500 mg tissue was homogenized in 2 ml distilled water; 1.6 ml of the homogenate was immediately transferred to 1.6 ml of 7% ice-cold perchloric acid. After extraction for 30 min, the samples were centrifuged to remove precipitated proteins, and the supernatant (3 ml) was neutralized by addition of 750 µl of 2.2-mol $KHCO_3$ for 30 min at room temperature and divided in two aliquots. The first aliquot was counted for total [^{3}H]-radioactivity. The second aliquot was passed through an anion exchange column (Ag-1 X8, Bio-Rad) to trap 2-DG-6-P. The column was eluted with 3 vol distilled water, which was counted for [^{3}H]-radioactivity. Because glucose-6-phosphatase activity is high in liver, we used 2-DG incorporation into glycogen as an index of glucose uptake.

Glycogen concentration. Glycogen concentration after KOH hydrolysis was measured microfluorometrically, as previously described (12). Briefly, dried tissue or glycogen precipitate was dissolved in 1N KOH (15 min, 55°C). After dilution with water (3 vol) the samples were buffered to pH 4.9 with HCl:Na-acetate buffer. The samples were then divided to aliquots and incubated with or without amyloglucosidase for 1 h at 37°C. Free and total glucose concentrations were measured microfluorometrically. The glucose derived from glycogen was calculated by dividing total glucose concentration by free glucose. All measurements were normalized for total protein concentration.

2-DG incorporation into glycogen. To assess 2-DG incorporation into glycogen, tissue samples (~50 mg) were crushed with mortar and pestle in liquid nitrogen, and the resulting powder was hydrolyzed in 500 µl 1N KOH for 15 min at 55°C. Once dissolved, the samples were chilled on ice. A 350-µl aliquot was pipetted in 2 vol prechilled 100% ethanol, and precipitation of macromolecules was allowed for 2 h at –20°C and followed by centrifugation (5,000 rpm, 30 min). The pellet was washed three times with 66% ethanol (–20°C). The dried pellet was dissolved in 100 µl of 1N KOH (55°C, 15 min), diluted with 300 µl distilled water, and buffered to pH 4.9 with 2 vol of 1:1 vol 0.25N HCl:0.15N Na-acetate, as previously described (12). A 1-ml sample was counted for [^{3}H]-radioactivity, and the remainder was measured microfluorometrically for glycogen concentration after amyloglucosidase treatment (12). The specific activity of glycogen was calculated by dividing the [^{3}H]-radioactivity by the respective glycogen concentration. Tissue glycogen synthesis from 2-DG was calculated by multiplying the glycogen specific activity by tissue glycogen concentration (see below) divided by the mean GSA.

Calculation of tissue-specific glucose uptake. The total of the [^{3}H]-radioactivity found in 2-DG-6-P and glycogen (dpm_{tot}) was divided by the mean specific activity of glucose during the study (120 min) to obtain the tissue-specific glucose uptake (nanomoles per milligram protein per minute). We performed additional experiments using subcutaneous injection of [^{14}C]deoxyglucose at 45 min in conjunction with the regular intraperitoneal 2-DG at 0 min to validate the use of intraperitoneal tracer administration. Administration of tracers by either approach gave essentially similar data. The ratio of ^{3}H to ^{14}C in 2-DG-6-P suggested that most of the 2-DG-6-P was accumulated during the last hour of the GTT. Both ways of administration resulted in a steady plasma specific activity of 2-DG/glucose.

Morphological analysis and insulin content of the pancreas. Animals were anesthetized by administering sodium aminobarbital, and pancreata were rapidly removed, cleared of fat and lymph nodes, weighed, and fixed in Bouin's solution for 4–6 h and transferred to 10% buffered formalin for 48 h before being embedded in paraffin. Sections were stained by hematoxylin and eosin. Pancreatic insulin content was measured by radioimmunoassay (Linco, St Louis, MO) using acid ethanol extracts of whole pancreases (10).

Analysis of body composition. Carcass analysis was performed as described (13), with minor modifications. Briefly, animals were weighed, then epididymal fat pads were dissected, weighed, and returned to the carcass. Carcasses were digested by alcoholic KOH hydrolysis at 60°C for 48 h. After saponification, the fat extract was neutralized and lipid content was determined by triglyceride assay (Sigma).

Statistical analysis. All statistical analyses were performed using unpaired Student's t test. A P value <0.05 was considered significant. Results are given as means ± SE.

RESULTS

Generation of βIRKO-MIRKO mice. βIRKO-MIRKO mice were generated by breeding βIRKO and MIRKO mice. The resulting study groups contained the four genotypes: control mice (IRlox/lox), MIRKO mice, βIRKO mice, and βIRKO-MIRKO mice. Both the single and double tissue-specific knockouts were heterozygous for the Cre transgene, as previously reported (9,10). We used the IRlox/lox as controls because glucose homeostasis has already been studied in these mice and was shown not to be different from that in their wild-type littermates (9,10). Because we bred F1 βIRKO and MIRKO littermates, all F2 mice studied were a homogeneously mixed genetic background. Mice were identified using a PCR strategy as detailed under RESEARCH DESIGN AND METHODS (Fig. 1*A*). Control mice, MIRKO mice, βIRKO mice, and βIRKO-MIRKO mice were born at the expected Mendelian frequency of 25% per genotype and showed similar size at birth and during the first 6–8 weeks of life. At 6 month of age, some βIRKO mice showed an 8% increase in body weight compared with controls ($P < 0.05$) and a 16 and 18% increase in body weight compared with βIRKO-MIRKO mice ($P < 0.0001$) and MIRKO mice ($P < 0.0001$), respectively (Fig. 1*B*).

βIRKO-MIRKO mice maintain normal fasting glucose and insulin levels. To assess the effects of simultaneous disruption of the IR in pancreatic β-cell and skeletal muscle on in vivo glucose metabolism, we measured fasting and random-fed glucose and insulin levels in controls, MIRKO, βIRKO, and βIRKO-MIRKO mice from 2 to 6 months of age. At 2 months of age, all four groups of mice exhibited comparable fasting and random fed blood glucose and insulin levels (data not shown). However, by 6 months of age, some βIRKO mice exhibited hyperglycemia and hyperinsulinemia, both in the fasting and fed states, compared with the other groups, and 18% had developed overt diabetes (defined as a fed glucose >250 mg/dl) (14) (Fig. 2*A–D*). Consistent with our previous findings (9), there were no significant differences in the fasting and fed blood glucose or insulin levels between MIRKO

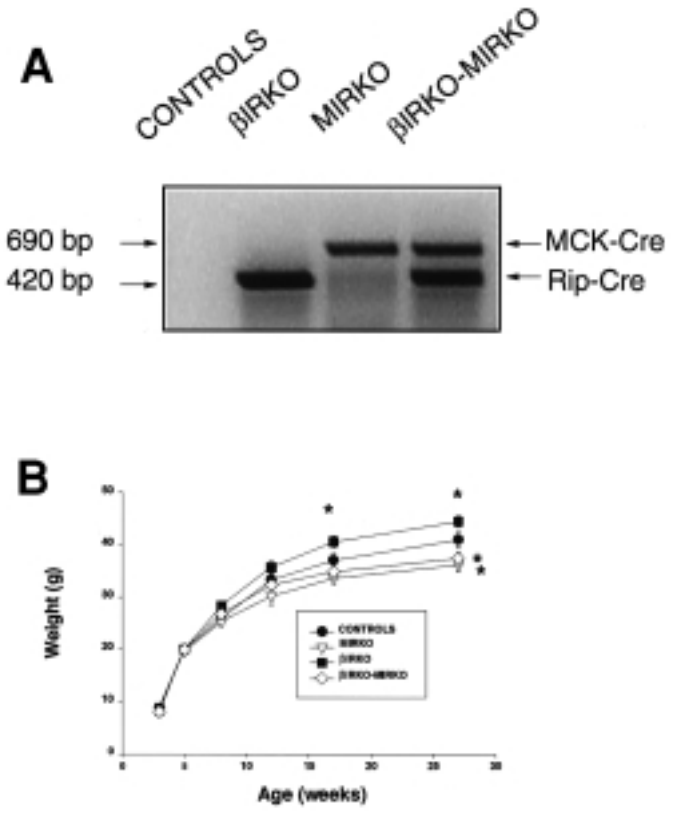

FIG. 1. Creation of BIRKO-MIRKO mice. *A*: mice were generated as detailed in RESEARCH DESIGN AND METHODS. DNA was extracted from tail biopsies and subjected to PCR analysis using the primers described. The presence of the RIP-*Cre* transgene in the βIRKO mice resulted in the presence of a 420-bp product; the presence of MCK-*Cre* transgene in the MIRKO mice resulted in a 690-bp product. In the βIRKO-MIRKO, both transgenes resulted in the amplification of both PCR products. *B*: Body weight of male controls, MIRKO, βIRKO, and βIRKO-MIRKO mice were determined at the indicated time points. Values represent the means ± SE of n = 28–32 mice per genotype. *P < 0.05; **P < 0.01, βIRKO vs. βIRKO-MIRKO.

and control mice. Compared with the βIRKO mice, however, the combined double knockout βIRKO-MIRKO mice maintained significantly lower glucose (P < 0.05) and insulin levels (P < 0.01), and only 7% of these mice developed overt diabetes (Fig. 2*A*–*D*).

βIRKO-MIRKO mice maintain a better glucose tolerance than βIRKO mice. Glucose tolerance was assessed in the four genotypes of mice between 2 and 6 months of age by intraperitoneal injection of glucose. Upon glucose challenge, the βIRKO mice exhibited an age-dependent progressive impairment of glucose tolerance, as previously described (10), whereas the MIRKO mice showed a very small increase in blood glucose (9) (Fig. 2*E* and *F*). βIRKO-MIRKO mice showed impaired glucose tolerance at both 2 and 6 months compared with control and MIRKO mice (AUC glucose [mg · dl^{-1} · min^{-1} · 1,000^{-1}] 2 months/6 months: 10.9/13.6, controls; 13/15.9, MIRKO; 17.2/25.1, βIRKO; 18.3/20.8, βIRKO-MIRKO; P < 0.01, βIRKO-MIRKO and βIRKO vs. controls and MIRKO at 2 and 6 months). However, consistent with the fasted and fed glucose levels, the hyperglycemia in the βIRKO-MIRKO mice during the IPGTT was less dramatic than in the βIRKO mice alone (Fig. 2*E* and *F*). During the IPGTT performed at 6 months of age, no significant difference was observed in insulin levels between MIRKO and control mice (Fig. 2*G*), whereas some βIRKO mice exhibited an approximately twofold increase in insulin levels in both the fasted state and 2 h into the GTT when compared with all other groups of mice (Fig. 2*G*). In contrast, double tissue-specific knockout βIRKO-MIRKO mice exhibited normal insulin levels in basal and stimulated states (Fig.2*G*). Thus, addition of a defect in muscle insulin action in βIRKO mice paradoxically improves both glucose tolerance and insulin levels compared with those in βIRKO mice, in both fasting and fed conditions and during a glucose challenge.

βIRKO-MIRKO mice are protected from loss of acute-phase insulin release. The loss of acute-phase insulin secretion in response to glucose contributes to glucose intolerance in the βIRKO mouse (10). Since βIRKO-MIRKO mice showed better glucose tolerance than βIRKO mice, we performed a correlation between acute-phase insulin release in response to glucose and glucose response of the corresponding individual mice during a standard IPGTT. In normal mice, we observed a three- to fourfold increase in insulin secretion 2 min after intraperitoneal glucose injection (3 g/kg body wt), corresponding to the peak of first-phase insulin release. This was followed by a 50% decrease at 5 min and then a gradual increase over 30 min, indicating a second-phase response (10). Under these conditions, ~80% of both control and MIRKO mice exhibited a typical peak of acute insulin release in response to glucose, whereas 20% failed to respond (Fig. 3*A*–*C*). Despite this difference, both responder and nonresponder groups had normal glucose tolerance to the intraperitoneal glucose challenge (compare filled circles and open triangles in Fig. 3*D* and *E*). In contrast to these results, and as previously noted (10), most of the βIRKO mice (72%) exhibited a loss of first-phase insulin release (P < 0.001) (Fig. 3*A* and *B*). Surprisingly, this number was reduced to only 46% in the βIRKO-MIRKO group (Fig. 3*A*). In both of these groups, loss of acute phase insulin release in response to glucose was a strong indicator of impaired glucose tolerance (Fig. 3*B*, *D*, and *E*). These data indicate that glucose-induced acute insulin release in βIRKO-MIRKO mice is significantly better than in βIRKO mice (P < 0.01) (Fig. 3*E*) and correlates with the improved glucose tolerance in these animals. One interpretation of this data is that the insulin resistance in muscle of βIRKO-MIRKO mice has a positive influence on glucose-stimulated first-phase insulin secretion from β-cells, suggesting some form of communication (via either substrates or hormones) between skeletal muscle and pancreatic β-cells.

To evaluate whether the differences in islet function are associated with altered islet morphology or capacity to produce and store insulin, we assessed islet size in pancreas sections of mice from all four groups at 6 months of age, using hematoxylin-eosin staining, and determined insulin content in acid ethanol extracts of pancreases. No difference in islet morphology (Fig. 4*A*) or in the pancreatic insulin content (Fig. 4*B*) could be detected between the four different genotypes of mice. It must be noted that βIRKO mice in this study are more hyperglycemic than originally reported and develop insulin resistance as they age. Indeed, some of them become obese and the altered islet morphology especially in these obese mice is in keeping with recent reports on a positive correlation between body weight and β-cell mass in rodents (15,16) Thus the phenotypic differences in

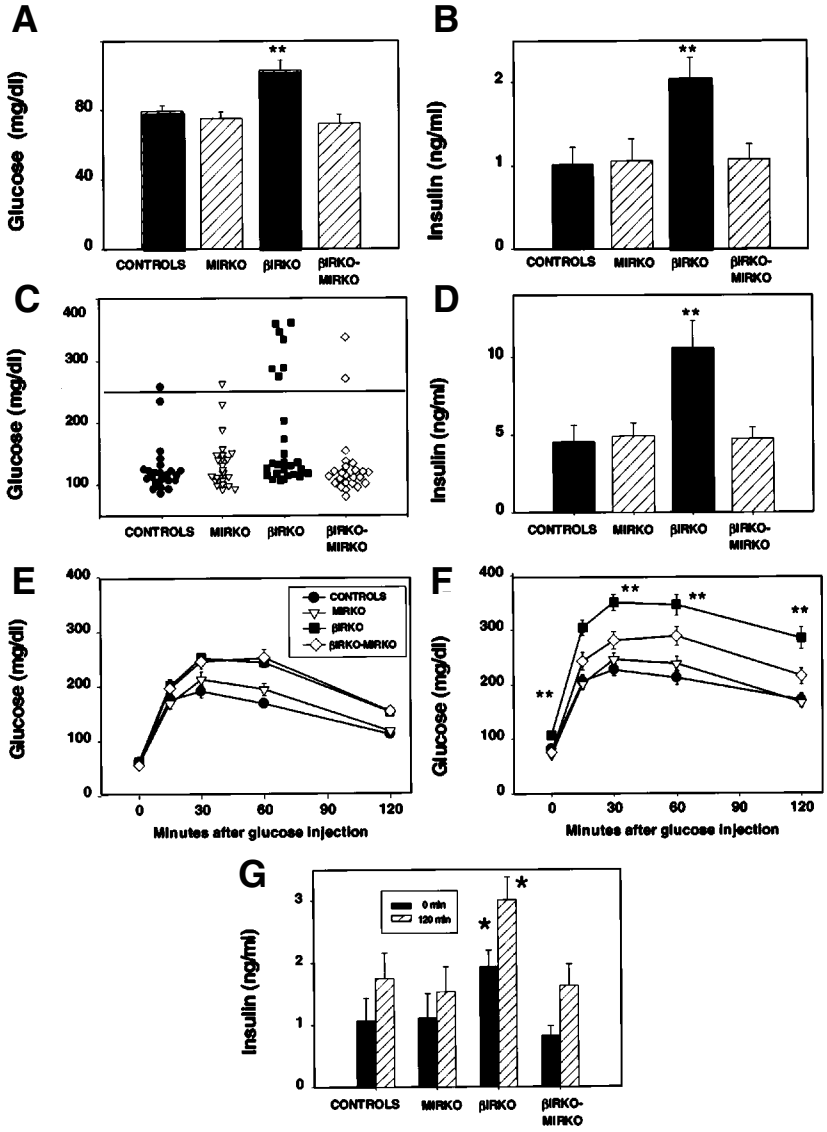

FIG. 2. βIRKO-MIRKO mice show relative improvement of glucose homeostasis. Fasting blood glucose (*A*) and insulin (*B*) levels and random fed blood glucose (*C*) and insulin (*D*) levels were determined in 6-month-old male controls, MIRKO, obese βIRKO, and βIRKO-MIRKO mice. Each bar represents the mean ± SE of n = 28–32 mice. **P < 0.01, βIRKO vs. βIRKO-MIRKO, MIRKO, or controls. GTT was performed in 2-month-old (*E*) and 6-month-old (*F*) male controls, MIRKO, obese βIRKO, and βIRKO-MIRKO mice by intraperitoneal injection of glucose (2 g/kg body wt). Results are expressed as means ± SE of n = 28–32 mice. *P < 0.05; **P < 0.01, βIRKO vs. βIRKO-MIRKO. Insulin levels during the GTT were determined by ELISA in 6-month-old mice of each genotype, both in the basal state and 120 min after glucose injection (*G*). Results are expressed as means ± SE of n = 13–19 mice. *P < 0.05, βIRKO vs. βIRKO-MIRKO.

some of the obese βIRKO mice may explain the relatively normal pancreas insulin content masking the overall phenotype of the group, as reported earlier (10).

Dynamic study of glucose uptake in vivo: 2-DG uptake and incorporation into glycogen during IPGTT. Glucose tolerance is dependent on multiple parameters, including glucose-induced insulin secretion and glucose uptake in insulin-sensitive tissues. Tissue-specific glucose uptake is usually determined during euglycemic clamp by giving an intravenous 2-DG tracer bolus, followed by determination of 2-DG plasma specific activity curve and measurement of 2-DG-6-P accumulation in the tissues of interest. This is possible because 2-DG is transported and phosphorylated but does not enter glycolysis (17,18). Because the input of 2-DG in tissues is reflected by its specific activity measured in the circulation, this technique does not necessarily require intravenous administration of the tracer. Thus, to determine the phenotype of MIRKO and βIRKO-MIRKO mice, we explored the fate of glucose under more physiological conditions, such as those of a glucose load. To further validate the intraperitoneal administration of 2-DG, 2-[^{14}C]deoxyglucose was also injected subcutaneously into the mice at 45 min into the GTT. Both routes of administration resulted in a steady plasma specific activity of 2-DG/glucose during the last hour of the experiment (Fig. 5*A*). Furthermore, 2-DG uptake in brain, a non–insulin-sensitive tissue, was identical in mice of all four genotypes (Fig. 5*B*), indicating the validity of the tracer as a measure of glucose uptake.

When this technique was applied to the study of glucose uptake in skeletal muscle, neither MIRKO nor βIRKO-MIRKO mice showed a significant change in 2-DG uptake compared with that in controls after 2 h, despite loss of insulin action in muscle (Fig. 5*C*), suggesting that most glucose entry over the 2-h test occurs via insulin-independent pathways. In βIRKO mice, 2-DG glucose uptake was slightly increased, probably reflecting the increased mass effect of glucose in these hyperglycemic animals (Fig. 5*C*). Indeed, when 2-DG glucose uptake in muscle was normalized for glucose AUC, no significant difference was detectable in the four groups of mice (data not shown). Despite the similarity in glucose uptake, glycogen content in muscle of MIRKO and βIRKO-MIRKO was decreased by 23 and 25% compared with that in both control and βIRKO mice (P < 0.05) (Fig. 5*D*). Thus, insulin resistance in mus-

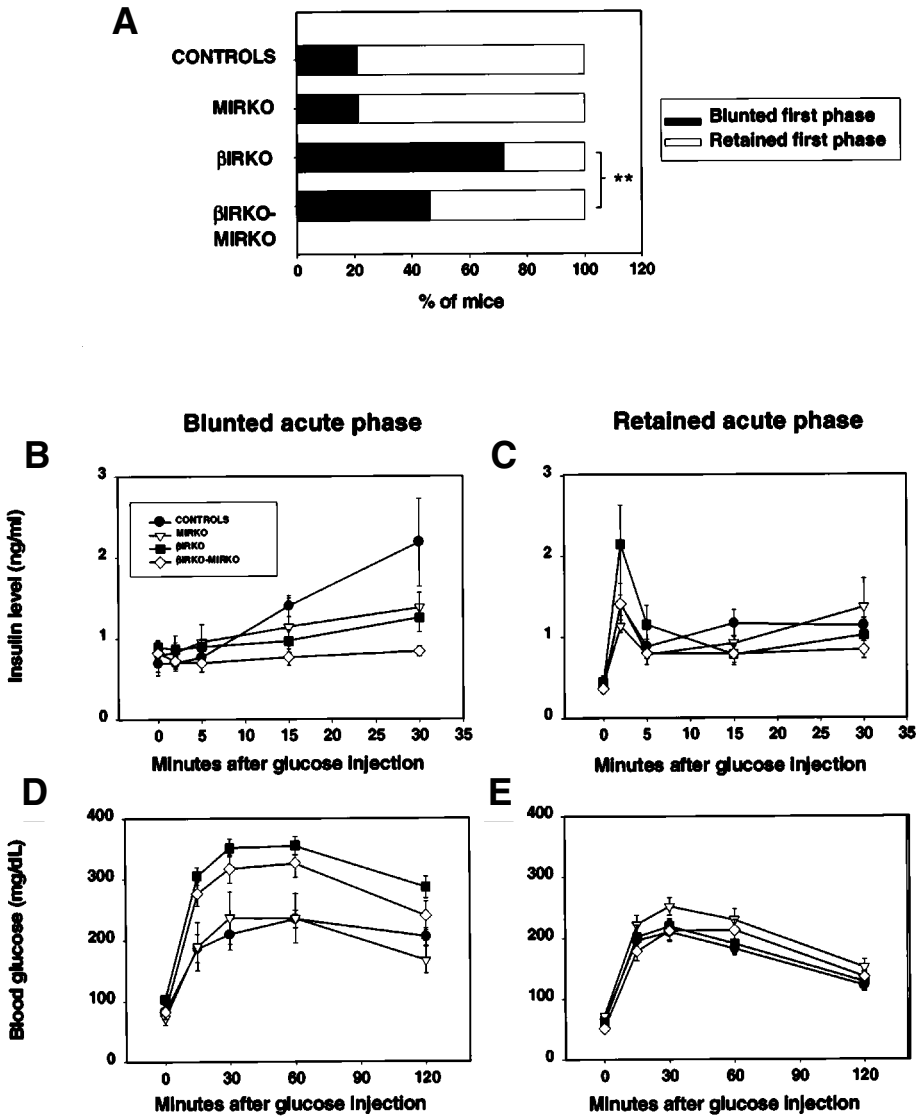

FIG. 3. βIRKO-MIRKO mice are protected from loss of acute phase insulin release. Acute-phase insulin release in response to glucose (3 g/kg i.p.) was studied in 3- to 4-month-old male mice of all groups, as detailed in RESEARCH DESIGN AND METHODS. *A* shows the percentage of mice with blunted or retained acute insulin release in response to glucose in each group (n = 28–32 mice per genotype). **$P < 0.01$, βIRKO vs. βIRKO-MIRKO (χ^2 test). The presence or absence of glucose-stimulated acute insulin release was determined in the same animals during a standard IPGTT (2g/kg). Insulin levels in mice with blunted versus retained acute insulin release are shown in *B* and *C*. *D* and *E* show the glucose responses in the same two groups of mice (n = 28–32 mice per genotype). All animals underwent each protocol on a different day in a random manner.

cle does not alter glucose uptake during physiological conditions but leads to impaired glucose storage, a characteristic finding in insulin-resistant states, including type 2 diabetes and obesity (19).

In contrast to the lack of change in total glucose uptake in muscle, both MIRKO and βIRKO-MIRKO mice showed a significant increase in 2-DG uptake in epididymal fat of 61 and 59%, respectively, compared with controls ($P < 0.05$, $P < 0.001$) (Fig. 6*A*). There were 35 and 33% increases compared with βIRKO mice ($P < 0.05$). βIRKO mice also showed a 21% increase in 2-DG uptake in fat compared with controls ($P < 0.05$), but this difference was not apparent when 2-DG uptake was normalized for glucose AUC (Fig. 6*B*). Most importantly, the higher 2-DG uptake in fat of MIRKO and βIRKO-MIRKO mice persisted after normalization for AUC and thus could not be explained by the hyperglycemia during the test (Fig. 6*B*).

Liver glycogen synthesis during the GTT, as measured by 2-DG incorporation into glycogen, was increased by 23, 45, and 44%, respectively, in MIRKO, βIRKO, and βIRKO-MIRKO mice compared with controls (Fig. 6*C*), while glycogen content was increased by 20–24% in MIRKO, βIRKO, and βIRKO-MIRKO mice compared with controls (Fig. 6*D*). Thus, during a glucose load, MIRKO and βIRKO-MIRKO mice show a significant shift of glucose utilization from muscle to fat and liver. This may explain in part the relatively normal glucose homeostasis of the MIRKO mice and the mild phenotype of the βIRKO-MIRKO mice.

Disturbances in lipid metabolism. Abnormalities in lipid metabolism can modulate insulin secretion and insulin action (20,21). Therefore, we assessed circulating lipid and leptin concentrations in the fasting state and determined body fat composition in the four groups of mice. No significant difference was found in the total cholesterol level among the four groups of mice. Triglyceride levels were increased by 40% in MIRKO mice, as previously described (9), and increased by 55% in the βIRKO and βIRKO-MIRKO mice (Table 1). Circulating FFAs also increased by 10–20% in all three groups of knockout mice, with the highest levels in the MIRKO and βIRKO-MIRKO mice (Table 1). Compared with controls, epididymal fat pad weight and total body fat (triglyceride content) were increased by 33–45% in MIRKO, βIRKO, and βIRKO-MIRKO mice (Table 1). Leptin concentrations were also modestly increased in MIRKO, βIRKO, and βIRKO-MIRKO mice, consistent with the increased fat content (Table 1).

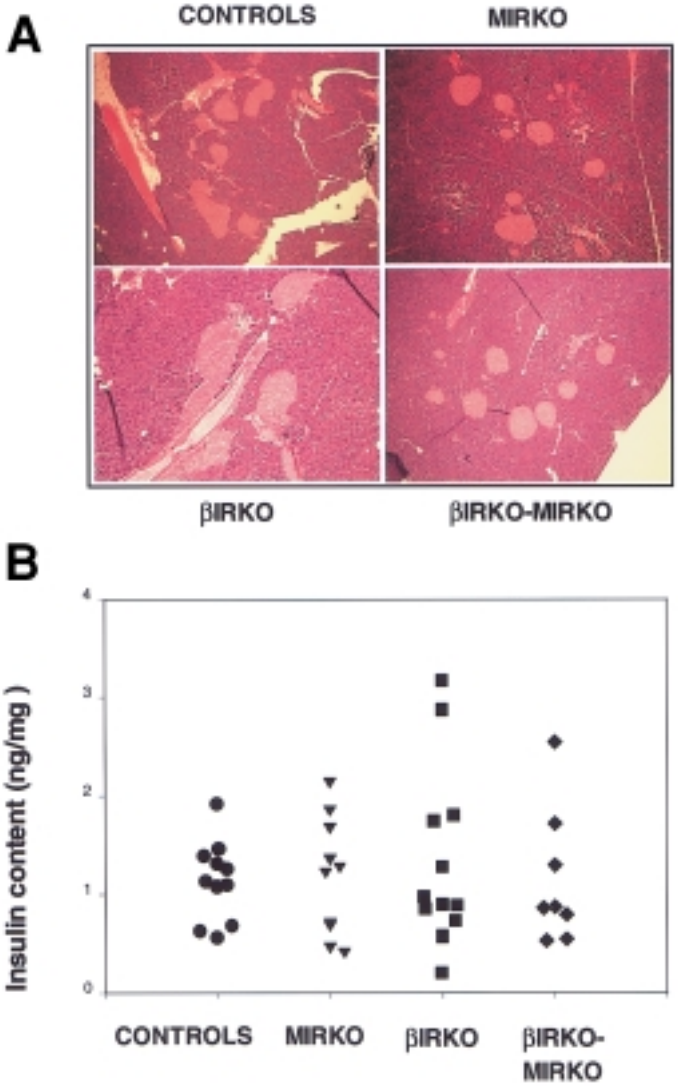

FIG. 4. Islet size and pancreas insulin content. *A*: Hematoxylin and eosin staining was performed on pancreas sections from 6-month-old male controls, MIRKO, obese βIRKO, and βIRKO-MIRKO mice. Representative sections are shown. *B*: Pancreas insulin content was measured in acid-ethanol extracts from 6-month-old male controls, MIRKO, obese βIRKO, and βIRKO-MIRKO mice. Data represent determinations for individual animals and are expressed in nanograms per milligram of pancreas (n = 4–6).

DISCUSSION

Type 2 diabetes is a multiorgan disease with alterations in insulin action in muscle, fat, and liver and decreased secretion of insulin from pancreatic β-cells. In this study, we have explored the interaction between insulin resistance in skeletal muscle and altered insulin secretion from pancreatic β-cells by developing a double tissue-specific insulin receptor knockout mouse. We have previously shown that isolated insulin resistance in muscle of MIRKO mice is insufficient to produce alterations in glucose tolerance, whereas loss of first-phase insulin secretion in βIRKO mice results in a marked impaired glucose tolerance (9,10). To our surprise, the βIRKO-MIRKO mice exhibit improved glucose homeostasis as well as normal fasting and fed glucose and insulin levels when compared with βIRKO mice alone.

Two different mechanisms may help explain these findings. First, in more than half the βIRKO-MIRKO mice there is a restoration of first-phase insulin secretion in response to glucose. Loss of first-phase insulin secretion in response to glucose is typical of the early stages of type 2 diabetes (22–24) and also occurs in the insulin-resistant β-cells of the βIRKO mouse (10). The molecular mechanism underlying increased β-cell responsiveness to glucose in the βIRKO-MIRKO mouse is not clear. Changes in pancreatic insulin synthesis do not seem to be the explanation because the morphology of the islets of Langerhans and the pancreas insulin content are the same in obese βIRKO and βIRKO-MIRKO mice. Stronger potential candidates are modulators of insulin secretion. Chronic exposure of the β-cells to elevated levels of FFAs has been shown to impair β-cell function and insulin secretion in vivo (20,25,26). However, FFA levels are similar in the three types of tissue-specific knockouts; thus, the differences in insulin secretion between the MIRKO mouse and the βIRKO mouse and the relative improvement of glucose sensing in the βIRKO-MIRKO mice cannot be accounted for by differences in FFA concentrations. Lactate released by muscle into the circulation might also modulate glucose sensing by β-cells (27,28); however, we did not detect any significant difference in lactate concentrations among the different groups of mice (data not shown). Likewise, although glucose toxicity may contribute to an acquired defect in insulin secretion of type 2 diabetic subjects (29,30), it is unlikely to be applicable in these mice because acute-phase insulin release studies were performed on 3-month-old mice, when fasted glucose levels between βIRKO and βIRKO-MIRKO mice are comparable. On the other hand, circulating leptin is increased in βIRKO mice, and leptin has been shown to inhibit insulin secretion in vitro and in vivo (31,32) via leptin receptors present on β-cells (33). Indeed, fasting leptin levels are lower in βIRKO-MIRKO mice than in βIRKO mice and could possibly contribute to the improvement in glucose sensing in the double knockout. Finally, muscle itself could release a factor that modulates β-cell function. The recently characterized α-endosulfine, which is expressed by muscle and inhibits K^+-sensitive ATP channels in β-cells, thereby potentiating glucose-induced insulin secretion, is one such candidate (34). All experimental animals used in this study were littermates obtained by multiple breeding to produce a mixed genetic background that might more closely represent human type 2 diabetes. The effect of modifier alleles is important in the development of type 2 diabetes and could potentially play a role in these animal models. By their very nature, tissue-specific knockout mice carry genes from at least three different mouse strains (C57 Bl, 129 Sv, and FVB). The role of this mixed genetic background in both pattern of substrate utilization and glucose sensing in βIRKO-MIRKO mice is impossible to predict. Thus, it is possible that the generation of βIRKO-MIRKO mice on a pure genetic background could either exaggerate the phenotype of βIRKO-MIRKO mice compared to βIRKO mice alone or attenuate it. Studies to investigate this issue and to identify these modifier genes are currently in progress.

The second mechanism demonstrated in this study that may contribute to protect the βIRKO-MIRKO mice from diabetes is a redistribution of substrates to other insulin-sensitive tissues. Glucose uptake in fat is increased by ~60% in MIRKO and βIRKO-MIRKO mice compared with controls, without concomitant increases in glucose or insulin concentrations.

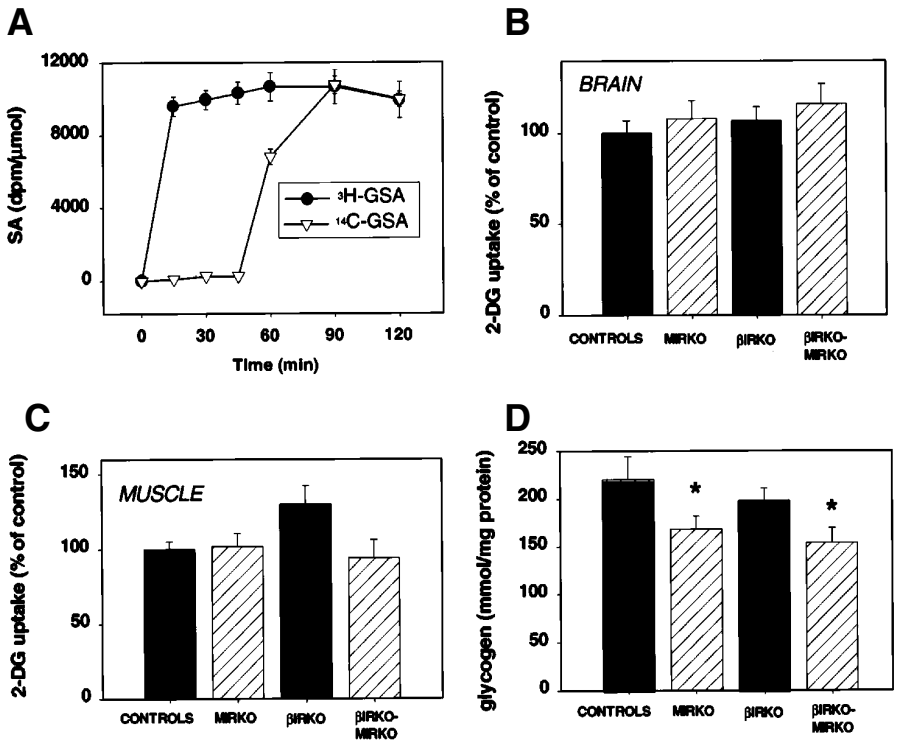

FIG. 5. Glucose uptake is maintained in muscle of MIRKO and βIRKO-MIRKO mice. Tissue-specific glucose uptake was studied in vivo during a GTT in 6-month-old controls, MIRKO, βIRKO, and βIRKO-MIRKO mice as described in RESEARCH DESIGN AND METHODS. To validate the intraperitoneal administration of 2-[^{3}H]deoxyglucose (0 min), 2-[^{14}C]deoxyglucose (in saline) was injected subcutaneously at 45 min. *A* shows the specific activity curves of 2-[^{3}H] and 2-[^{14}C]deoxyglucose in plasma. 2-DG uptake in brain (*B*) and muscle (*C*) is expressed relative to that in controls in each experiment (n = 12 per genotype). Glycogen content was determined in skeletal muscle of 6-month-old random-fed mice (*D*). Results are expressed as means ± SE of n = 8 mice per genotype. *P < 0.05, MIRKO and βIRKO-MIRKO vs. controls.

Thus, both MIRKO and βIRKO-MIRKO mice show a significant shift of glucose uptake from muscle to fat. During euglycemic-hyperinsulinemic clamps, MIRKO mice show a threefold increase in glucose utilization in adipose tissue, consistent with a sensitization to insulin (35). The increased glucose uptake in fat may in part explain the maintenance of euglycemia in MIRKO mice, the protection from development of diabetes in βIRKO-MIRKO mice, and the increased adiposity seen in both of these groups. In this way, decreased glucose uptake in muscle may promote glucose uptake and triglyceride storage in adipose tissue, predisposing to obesity. Consequently, increased fat mass may secrete various modulators of insulin sensitivity, such as FFA, leptin, or tumor necrosis factor-α (36), that can lead to additional insulin resistance in liver and fat. This model is consistent with previous studies in the Zucker rat, in which obesity is associated with early insulin

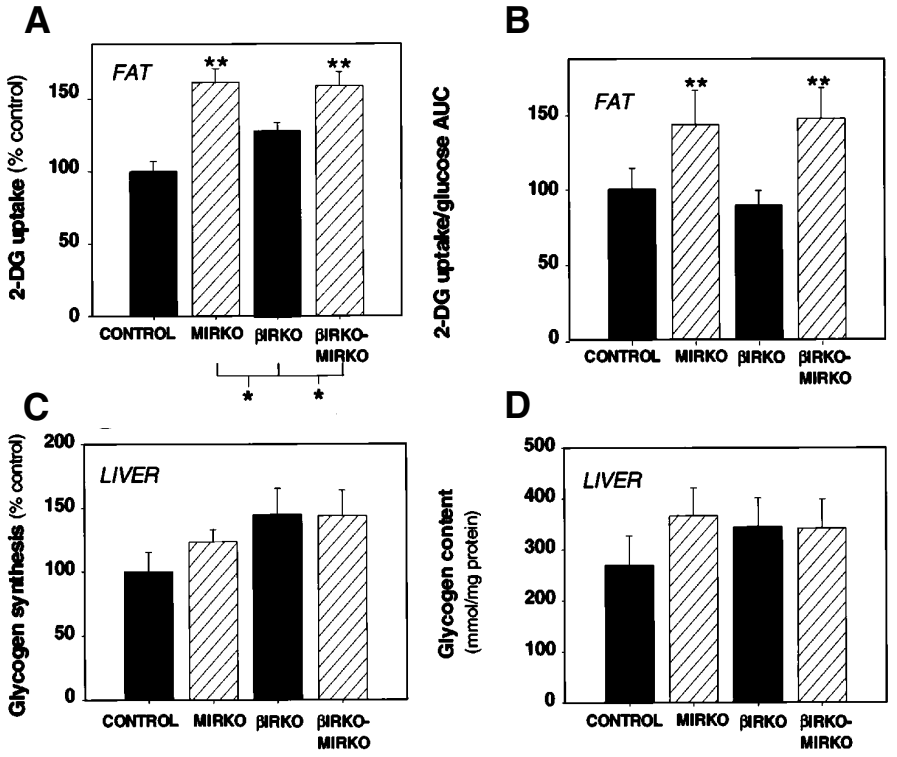

FIG. 6. Glucose shunting toward fat and liver in MIRKO and βIRKO-MIRKO mice. *A*: 2-DG uptake in fat in 6-month-old male mice of all genotypes is expressed as mean ± SE of relative 2-DG uptake (percentage of controls) in each experiment (n = 12). *P < 0.05; **P < 0.01, MIRKO and βIRKO-MIRKO vs. βIRKO and controls. *B*: 2-DG uptake in fat normalized for glycemia was obtained by dividing the fat 2-DG uptake by the AUC of glucose during the experiment. *P < 0.05; **P < 0.01, MIRKO and βIRKO-MIRKO vs. βIRKO and controls. *C*: Liver glycogen synthesis was measured by 2-DG incorporation into glycogen during GTT. Values are expressed in relative glycogen synthesis (percentage of controls) in each experiment (n = 9). *D*: Liver glycogen content was assessed as described in RESEARCH DESIGN AND METHODS. Values represent the means ± SE of n = 6 mice.

TABLE 1
Parameters of lipid metabolism

	Plasma lipids			Epididymal fat weight (% body wt)	Triglyceride content (% body wt)	Serum leptin (ng/ml)
	Cholesterol (mg/dl)	Triglycerides (mg/dl)	FFAs (meq/dl)			
Controls	99.5 ± 2.5	115.7 ± 13	1,376 ± 64	3.57 ± 0.2	27.5 ± 2.3	12.14 ± 2.3
MIRKO	101.2 ± 3.2	165.1 ± 14*	1,594 ± 58*	4.74 ± 0.2*	38 ± 6.4†	14.6 ± 3.0
βIRKO	99.8 ± 4.2	179 ± 19*	1,531 ± 57	4.59 ± 0.4*	35.7 ± 3.6†	25.9 ± 3.1†
βIRKO-MIRKO	102.5 ± 5.6	179.7 ± 13*	1,662 ± 102*	5.2 ± 0.4*	38.6 ± 6.9*	17.3 ± 2.3

Data are means ± SE for $n = 3$ individual mice in each group. The βIRKO group consists of both obese and nonobese mice. *$P < 0.05$, †$P < 0.01$ vs. controls.

resistance in muscle, although insulin sensitivity in white adipose tissue remains normal (37).

The exact mechanism for this communication between muscle and adipocytes remains unclear. In vitro insulin-stimulated glucose uptake in isolated adipocytes from MIRKO and βIRKO-MIRKO mice is not significantly different from that in adipocytes from controls (data not shown). Likewise, the expression level of the glucose transporters GLUT1 and GLUT4 in fat is unchanged between the different groups of mice (data not shown). Thus, as in the case of the β-cells, the modifications of adipocyte metabolism may depend on a circulating factor that regulates glucose uptake or metabolism in vivo. Liver glycogen synthesis is also increased in all three knockout mice compared with controls. In the βIRKO mice, this may be due to hyperglycemia, since hyperglycemia per se is a stimulator of glycogen synthesis and an inhibitor of glycogenolysis (38). However, the MIRKO and βIRKO-MIRKO mice used in this experiment were not hyperglycemic, suggesting that increased liver glycogen synthesis may also reflect a modulatory role of muscle insulin resistance on glucose uptake by other insulin-sensitive tissues.

Using labeled deoxyglucose, we surprisingly observed that glucose uptake in muscle of MIRKO and βIRKO-MIRKO mice approximates normal during a glucose load. Thus, it appears that in mice, the majority of glucose uptake occurring in skeletal muscle in the postprandial state is not insulin dependent. This provides a partial explanation as to why MIRKO mice are not overtly insulin resistant or glucose intolerant. Contraction of muscles could be an explanation for this finding because exercise can activate postreceptor insulin signaling and increase glucose transport in muscle from MIRKO mice independently of insulin (39). It is also possible that glucose uptake in muscle is triggered by insulin-dependent mechanisms acting through another cell type indirectly on muscle fiber (such as NO or cGMP acting on muscle to enhance glucose uptake) (40,41). This finding (e.g., maintenance of glucose uptake in MIRKO muscle) appears discordant with previous hyperinsulinemic clamp studies that suggest that insulin-mediated glucose utilization by muscle represents up to 80% of the glucose infused (42) and that insulin resistance in skeletal muscle accounts for the impairment in glucose uptake in type 2 diabetes (43–46). Indeed, MIRKO mice show reduced glucose uptake in skeletal muscle during euglycemic-hyperinsulinemic clamp studies, as shown by Shulman and coworkers (35). However, one should keep in mind that under the hyperinsulinemic conditions of the clamp, the infused glucose is driven preferentially into muscle and only the insulin-dependent fraction of glucose uptake is explored; therefore, muscle insulin resistance is easily detectable. In MIRKO mice, insulin resistance at steps other than glucose uptake probably accounts for the decrease in muscle glycogen content. Thus, although glucose uptake is largely rate-limiting for glycogen synthesis, defective insulin signaling can lead to decreases in nonoxidative metabolism, such as those seen in type 2 diabetes (19). Taken together, these finding suggest that the role of insulin action in muscle is more to promote glucose storage than to promote glucose uptake.

In summary, βIRKO-MIRKO mice show improved glucose homeostasis compared with βIRKO mice. The defect in insulin action in muscle of βIRKO-MIRKO mice does not significantly alter the ability of muscle to handle a glucose load, but it protects β-cell function and increases uptake of glucose by adipose tissue and liver. These data suggest that *1*) defective insulin signaling in muscle can lead to decreased glycogen storage, despite normal glucose uptake; *2*) muscle may act as a regulator of glucose uptake/metabolism in other insulin-sensitive tissues and in β-cells, possibly by endocrine or metabolic mechanisms; and *3*) primary insulin resistance in muscle may lead to increased adiposity and development of obesity. The βIRKO-MIRKO mouse provides new insights into the role of skeletal muscle in the regulation of glucose homeostasis and represents an interesting model to investigate the pathogenesis of obesity and type 2 diabetes.

ACKNOWLEDGMENTS

This work was supported by National Institutes of Health (NIH) Grant DK31036 (C.R.K.), Joslin Diabetes Endocrinology Research Center Project Grant DK36836 (C.R.K.), NIH National Research Service Award DK09825-02 (R.N.K), and NIH National Research Service Award DK09817-02 (M.D.M.). A.V. was supported by a grant from the Sigrid Juselius Foundation, the Livoch Halsa Foundation.

We thank K.E. Miller for her technical assistance during metabolic studies and O. Peroni and B.B. Kahn for their help and advice on in vitro glucose uptake in isolated adipocytes. We are also grateful to J. Konigsberg and T.L. Azar for their expert assistance in preparing this manuscript.

REFERENCES

1. DeFronzo RA: The triumvirate: β-cell, muscle, liver: a collusion responsible for NIDDM (Lilly Lecture). *Diabetes* 37:667–687, 1988
2. Kahn CR: Insulin action, diabetogenes, and the cause of type II diabetes (Banting Lecture). *Diabetes* 43:1066–1084, 1994
3. Gepts W, Lecompte PM: The pancreatic islets in diabetes. *Am J Med* 70:105–115, 1981
4. Accili D, Drago J, Lee EJ, Johnson MD, Cool MH, Salvatore P, Asico LD, Jose PA, Taylor SI, Westphal HD: Early neonatal death in mice homozygous for a null allele of the insulin receptor gene. *Nat Genet* 12:106–109, 1996

5. Araki E, Lipes MA, Patti ME, Brüning JC, Haag BL III, Johnson RS, Kahn CR: Alternative pathway of insulin signalling in mice with targeted disruption of the IRS-1 gene. *Nature* 372:186–190, 1994
6. Tamemoto H, Kadowaki T, Tobe K, Yagi T, Sakura H, Hayakawa T, Terauchi Y, Ueki K, Kaburagi Y, Satoh S, Sekihara H, Yoshioka S, Horikoshi H, Furuta Y, Ikawa Y, Kasuga M, Yazaki Y, Aizawa S: Insulin resistance and growth retardation in mice lacking insulin receptor substrate-1. *Nature* 372:182–186, 1994
7. Withers DJ, Gutierrez JS, Towery H, Burks DJ, Ren JM, Previs S, Zhang Y, Bernal D, Pons S, Shulman GI, Bonner-Weir S, White MF: Disruption of IRS-2 causes type 2 diabetes in mice. *Nature* 391:900–904, 1998
8. Katz EB, Stenbit AE, Hatton K, DePinho RA, Charron MJ: Cardiac and adipose tissue abnormalities but not diabetes in mice deficient in GLUT4. *Nature* 377:151–155, 1995
9. Bruning JC, Michael MD, Winnay JN, Hayashi T, Horsch D, Accili D, Goodyear LJ, Kahn CR: A muscle-specific insulin receptor knockout exhibits features of the metabolic syndrome of NIDDM without altering glucose tolerance. *Mol Cell* 2:559–569, 1998
10. Kulkarni RN, Bruning JC, Winnay JN, Postic C, Magnuson MA, Kahn CR: Tissue-specific knockout of the insulin receptor in pancreatic β cells creates an insulin secretory defect similar to that in type 2 diabetes. *Cell* 96:329–339, 1999
11. Passonneau JV, Lowry OH: *Enzymatic Analysis: A Practical Guide*. Ottawa, ON, Canada, Humana Press, 1993
12. Virkamaki A, Rissanen E, Hamalainen S, Utriainen T, Yki-Jarvinen H: Incorporation of [$^{3\text{-}3}$H]glucose and 2-[$^{1\text{-}14}$C]deoxyglucose into glycogen in heart and skeletal muscle in vivo: implications for the quantitation of tissue glucose uptake. *Diabetes* 46:1106–1110, 1997
13. Moller DE, Chang PY, Yaspelkis BB III, Flier JS, Wallberg-Henriksson H, Ivy JL: Transgenic mice with muscle-specific insulin resistance develop increased adiposity, impaired glucose tolerance, and dyslipidemia. *Endocrinology* 137: 2397–2405, 1996
14. Bruning JC, Winnay J, Bonner-Weir S, Taylor SI, Accili D, Kahn CR: Development of a novel polygenic model of NIDDM in mice heterozygous for IR and IRS-1 null alleles. *Cell* 88:561–572, 1997
15. Bonner-Weir S: Islet growth and development in the adult. *J Mol Endocrinol* 24:297–302, 2000
16. Montanya E, Nacher V, Biarnes M, Soler J: Linear correlation between β-cell mass and body weight throughout the life span in Lewis rats: role of β-cell hyperplasia and hypertrophy. *Diabetes* 49:1341–1346, 2000
17. Hom FG, Goodner CJ, Berrie MA: A [^{3}H]2-deoxyglucose method for comparing rates of glucose metabolism and insulin responses among rat tissues in vivo: validation of the model and the absence of an insulin effect on brain. *Diabetes* 33:141–152, 1984
18. Ferré P, Burnol AF, Leturque A, Terretaz J, Penicaud L, Jeanrenaud B, Girard J: Glucose utilization in vivo and insulin-sensitivity of rat brown adipose tissue in various physiological and pathological conditions. *Biochem J* 233:249–252, 1986
19. Golay A, Felber JP, Jequier E, DeFronzo RA, Ferrannini E: Metabolic basis of obesity and noninsulin-dependent diabetes mellitus. *Diabetes Metab Rev* 4:727–747, 1988
20. Unger RH: Lipotoxicity in the pathogenesis of obesity-dependent NIDDM: genetic and clinical implications. *Diabetes* 44:863–870, 1995
21. Lupi R, Marchetti P, Maffei M, Del Guerra S, Benzi L, Marselli L, Bertacca A, Navalesi R: Effects of acute or prolonged exposure to human leptin on isolated human islet function. *Biochem Biophys Res Commun* 256:637–641, 1999
22. Cerasi E, Luft R, Efendic S: Decreased sensitivity of the pancreatic beta cells to glucose in prediabetic and diabetic subjects: a glucose dose-response study. *Diabetes* 21:224–234, 1972
23. Polonsky KS: The beta-cell in diabetes: from molecular genetics to clinical research (Lilly Lecture). *Diabetes* 44:705–717, 1995
24. Efendic S, Grill V, Luft R, Wajngot A: Low insulin response: a marker of prediabetes. *Adv Exp Med Biol* 246:167–174, 1988
25. Man AW, Zhu M, Noma Y, Toide K, Sato T, Asahi Y, Hirashima T, Mori S, Kawano K, Mizuno A, Sano T, Shima K: Impaired β-cell function and deposition of fat droplets in the pancreas as a consequence of hypertriglyceridemia in OLETF rat, a model of spontaneous NIDDM. *Diabetes* 46:1718–1724, 1997
26. Mason TM, Goh T, Tchipashvili V, Sandhu H, Gupta N, Lewis GF, Giacca A: Prolonged elevation of plasma free fatty acids desensitizes the insulin secretory response to glucose in vivo in rats. *Diabetes* 48:524–530, 1999
27. Zhao C, Rutter GA: Overexpression of lactate dehydrogenase A attenuates glucose-induced insulin secretion in stable MIN-6 beta-cell lines. *FEBS Lett* 430:213–216, 1999
28. Salgado AP, Pereira FC, Seica RM, Fernandes AP, Flatt PR, Santos RM, Rosario LM, Ramasamy R: Modulation of glucose-induced insulin secretion by cytosolic redox state in clonal beta-cells. *Mol Cell Endocrinol* 154:79–88, 1999
29. Rossetti L, Giaccari A, DeFronzo RA: Glucose toxicity. *Diabetes Care* 13:610–630, 1990
30. Leahy JL: Natural history of beta cell dysfunction in non-insulin-dependent diabetes mellitus. *Diabetes Care* 13:992–1010, 1990
31. Seufert J, Kieffer TJ, Habener JF: Leptin inhibits insulin gene transcription and reverses hyperinsulinemia in leptin-deficient ob/ob mice. *Proc Natl Acad Sci U S A* 96:674–679, 1999
32. Kulkarni RN, Wang ZL, Wang RM, Hurley JD, Smith DM, Ghatei MA, Withers DJ, Gardiner JV, Bailey CJ, Bloom SR: Leptin rapidly suppresses insulin release from insulinoma cells, rat and human islets and, *in vivo*, in mice. *J Clin Invest* 100:2729–2736, 1997
33. Kieffer TJ, Heller RS, Habener JF: Leptin receptors expressed on pancreatic beta-cells. *Biochem Biophys Res Commun* 224:522–527, 1996
34. Heron L, Virsolvy A, Peyrollier K, Gribble FM, Le Cam A, Ashcroft FM, Bataille D: Human alpha-endosulfine, a possible regulator of sulfonylurea-sensitive KATP channel: molecular cloning, expression and biological properties. *Proc Natl Acad Sci U S A* 95:8387–8391, 1998
35. Kim JK, Michael MD, Previs SF, Mauvais-Jarvis F, Kahn CR, Shulman GI: Redistribution of substrates to adipose tissue in mice with selective insulin resistance in muscle promotes obesity. *J Clin Invest* 105:1791–1797, 2000
36. Hotamisligil GS, Shargill NS, Spiegelman BM: Adipose expression of tumor necrosis factor-α: direct role in obesity-linked insulin resistance. *Science* 259:87–91, 1993
37. Penicaud L, Ferre P, Terretaz J, Kinebanyan MF, Leturque A, Dore E, Girard J, Jeanrenaud B, Picon L: Development of obesity in Zucker rats: early insulin resistance in muscles but normal sensitivity in white adipose tissue. *Diabetes* 36:626–631, 1987
38. Bollen M, Keppens S, Stalmans W: Specific features of glycogen metabolism in the liver. *Biochem J* 336:19–31, 1998
39. Wojtaszewski JFP, Higaki Y, Hirshman MF, Michael MD, Dufresne SD, Kahn CR: Exercise modulates postreceptor insulin signaling and glucose transport in muscle-specific insulin receptor knockout mice. *J Clin Invest* 104:1257–1264, 1999
40. Etgen GJ Jr, Fryburg DA, Gibbs EM: Nitric oxide stimulates skeletal muscle glucose transport through a calcium/contraction- and phosphatidylinositol-3-kinase-independent pathway. *Diabetes* 46:1915–1919, 1997
41. Young ME, Radd GK, Leighton B: Nitric oxide stimulates glucose transport and metabolism in rat skeletal muscle *in vitro*. *Biochem J* 322:223–228, 1997
42. DeFronzo RA, Jacot E, Jequier E, Maeder E, Wahren J, Felber JP: The effect of insulin on the disposal of intravenous glucose: results from indirect calorimetry and hepatic and femoral venous catheterization. *Diabetes* 30: 1000–1007, 1981
43. DeFronzo RA, Gunnarsson R, Bjorkman O, Olsson M, Wahren J: Effects of insulin on peripheral and splanchnic glucose metabolism in non-insulin dependent diabetes mellitus. *J Clin Invest* 76:149–155, 1985
44. DeFronzo RA: Pathogenesis of type 2 (non-insulin-dependent) diabetes mellitus: a balanced overview. *Diabetologia* 35:389–397, 1992
45. Lillioja S, Mott DM, Spraul M, Ferraro R, Foley JE, Ravussin E, Knowler WC, Bennett PH, Bogardus C: Insulin resistance and insulin secretory dysfunction as precursors of non-insulin-dependent diabetes mellitus: prospective studies of Pima Indians. *N Engl J Med* 329:1988–1992, 1993
46. Bogardus C: Insulin resistance in the pathogenesis of NIDDM in Pima Indians. *Diabetes Care* 16:228–231, 1993